(Preprint) AAS 11-444

METHODOLOGY AND RESULTS OF THE NEAR-EARTH OBJECT (NEO) HUMAN SPACE FLIGHT (HSF) ACCESSIBLE TARGETS STUDY (NHATS)

Brent W. Barbee*, Ronald G. Mink†, Daniel R. Adamo‡, and Cassandra M. Alberding§

Near-Earth Asteroids (NEAs) have been identified by the Administration as potential destinations for human explorers during the mid-2020s. Planning such ambitious missions requires selecting potentially accessible targets from the growing known population of 8,008 NEAs. NASA is therefore conducting the Near-Earth Object (NEO) Human Space Flight (HSF) Accessible Targets Study (NHATS), in which the trajectory opportunities to all known NEAs are being systematically evaluated with respect to a set of defined constraints. While the NHATS algorithms have identified hundreds of NEAs which satisfy purposely inclusive trajectory constraints, only a handful of them offer truly attractive mission opportunities in the time frame of greatest interest. In this paper we will describe the structure of the NHATS algorithms and the constraints utilized in the study, present current study results, and discuss various mission design considerations for future human space flight missions to NEAs.

INTRODUCTION

Near-Earth objects (NEOs) are asteroids and comets with perihelion distance < 1.3 AU, permitting many of them to closely approach or cross Earth's orbit. The vast majority of NEOs are asteroids, classified as near-Earth asteroids (NEAs). These objects are largely unchanged since the early days of our solar system and may have even deposited the seeds of life on the young Earth; studying them therefore provides vital scientific knowledge about the formation and evolution of both the solar system and our own planet. However, there is evidence of many past impacts on Earth by these objects, some of which were sufficiently energetic to destroy life on a planetary scale. These objects therefore bear careful monitoring for the possibility of future impacts that we would hopefully be able to prevent. The close proximity of some of these objects' orbits to Earth's orbit and the fact that some of them contain usable resources, such as water, raises the possibility of sending human explorers to visit them. While that is the primary focus of this paper, it is important to recognize that the study and exploration of NEAs is simultaneously motivated by fundamental science, planetary defense against impacts, and human space exploration.

NEAs have been identified by the current presidential administration as potential destinations for human explorers during the mid-2020s. While the close proximity of these objects' orbits to Earth's orbit creates the aforementioned risk of highly damaging or catastrophic impacts, it also makes some of these objects potentially accessible to spacecraft departing from and returning to Earth; this presents unique opportunities for solar system science and humanity's first ventures beyond cislunar space.

The planning and execution of such ambitious missions presents formidable technical, programmatic, and political challenges. The first challenge, which is of a technical nature, is to develop and implement a process capable of identifying potentially accessible targets from within the large and growing known population of

*Aerospace Engineer, NASA GSFC, Code 595, 8800 Greenbelt Road, Greenbelt, MD 20771, USA. Member AIAA.
†Mission Systems Engineer, NASA GSFC, Code 592, 8800 Greenbelt Road, Greenbelt, MD 20771, USA.
‡Astrodynamics Consultant, 4203 Moonlight Shadow Ct., Houston, TX 77059, USA. Senior Member AIAA.
§Aerospace Engineer, NASA GSFC, Code 595, 8800 Greenbelt Road, Greenbelt, MD 20771, USA.

8,038 NEAs*. To accomplish this, NASA is conducting the Near-Earth Object (NEO) Human Space Flight (HSF) Accessible Targets Study (NHATS). Phase I of the NHATS was executed during September of 2010, and Phase II was completed by early March of 2011. Both phases of the study considered only NEAs; near-Earth comets (NECs) were not included because their orbits are typically more difficult to reach due to their very high eccentricities and long periods, and because their active nature could create a hazardous environment for a human crew. The NHATS is ongoing because previously undetected NEAs are being discovered constantly and the ephemerides of known NEOs are updated when new observations are incorporated into the orbit determination process. These factors have motivated an effort to automate the analysis process in order to provide continuous monitoring of NEA accessibility.

The NHATS analysis process consists of a trajectory filter and a minimum estimated size criterion. The trajectory filter employs the method of embedded trajectory grids[1] to compute all possible ballistic round-trip mission trajectories to every NEA in the Jet Propulsion Laboratory (JPL) Small-Body Database (SBDB); all round-trip trajectory solutions that satisfy the trajectory filter criteria are stored. An NEA must offer at least one qualifying trajectory solution to pass the trajectory filter, and it's estimated size must be greater than or equal to the minimum estimated size criterion. The trajectory filter criteria are purposely inclusive, and the estimated size criteria is based on a notional lower limit for NEA albedo, making it an optimistic estimated size and therefore also inclusive. The inclusive nature of the NHATS constraints on trajectory performance and object size is motivated by the desire to obtain a sufficiently comprehensive view of the NEA accessibility landscape before down-selecting candidate targets. This comprehensive view provides useful context and helps to inform current research efforts towards a dynamical theory of round-trip accessibility for NEAs.

While the NHATS has identified hundreds of NEAs which pass the purposely inclusive trajectory filter and meet minimum estimated size constraints which are arguably rather small (30 - 50 m), only a few of these offer potentially attractive mission opportunities during the time frame of greatest interest (mid-2020s to mid-2030s). However, it must be stressed that NASA considers the NHATS results to be pre-decisional as potentially accessible trajectory solutions are only one factor of many in the design and consideration of a future human space flight program. Moreover, the actual NEA population $\geq$ 30 m is likely to consist of at least several tens of thousands of members, and quite possibly more (hundreds of thousands or even millions), of which we have discovered $<$ 9,000. This has led the technical community concerned with NEOs to recommend the deployment of a space-based NEO survey telescope which would avoid the geometrical constraints associated with observing solely from Earth and thus provide a very comprehensive NEO population survey within only a few years of deployment.[2] Such a survey would simultaneously benefit the scientific, HSF, and planetary defense communities.

In this paper we will describe and discuss the workings of the NHATS algorithms, the assumptions built into their operation, and the constraints selected for the study. We will then present the results of the NHATS to date and discuss the trends and features of the data. The ongoing and future work for the project will also be discussed.

MISSION PHASES

Certain fundamental assumptions about mission design had to be made in order to perform round-trip trajectory calculations over billions of combinations of Earth departure dates and trajectory segment flight times for thousands of NEAs. Assumptions were limited to only those which are necessary for Δv calculations; no assumptions were made regarding specific mission architecture elements such as the types of propulsion systems used, the masses of vehicle elements, or the performance capabilities of launch vehicles. In the future it may be possible to define a realistic reference architecture that would permit the computation of Initial Mass in Low Earth Orbit (IMLEO) and the attendant number of required launches, but the forward path for Human Space Flight (HSF) architecture is currently too uncertain to make such a calculation meaningful.

Nevertheless, the basic segments of a HSF mission to a NEO are reasonably well defined. As shown in Figure 1, the spacecraft will depart Earth by performing some Earth departure maneuver which places the

*This population number is current as of 07/19/2011. Population statistics are continually updated at `http://neo.jpl.nasa.gov/stats/`

spacecraft onto a heliocentric trajectory that intercepts the NEO some time later. Upon intercepting the NEO, the spacecraft will then perform a velocity change maneuver to match the NEO's heliocentric velocity. After remaining in the vicinity of the NEO for some period of time, the spacecraft will change its velocity so as to place it onto a heliocentric orbit that will intercept the Earth some time later. Upon arrival at Earth, the spacecraft may have to perform a final maneuver to reduce its velocity with respect to the Earth.

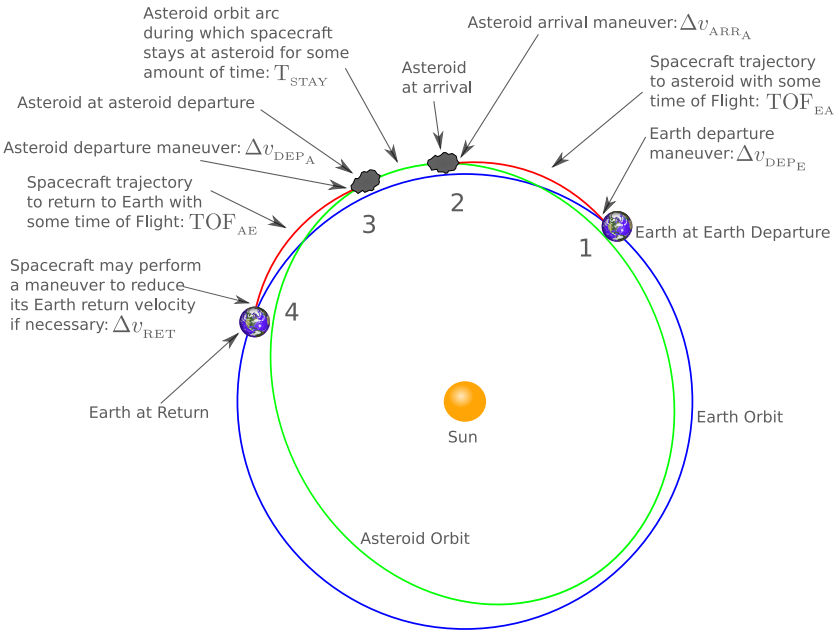

Figure 1. Profile of an HSF Mission to a NEO

The NEO arrival and departure maneuvers are quite straightforward, but certain assumptions were required to compute Earth departure and Earth return maneuvers. These assumptions and their rationale are discussed in the sections that follow.

Earth Departure

The nature of the spacecraft's Earth departure maneuver, which may be referred to as Trans-NEO Injection (TNI), depends on the architecture and concept of operations for the mission. While the design of the spacecraft and the way in which it departs Earth may vary, it is almost certain that the total required spacecraft mass cannot be assembled on Earth's surface and delivered to orbit using only a single launch. Thus the spacecraft will have to be assembled in space and then depart from a particular parking orbit. Assembly could be as simple as launching the crew vehicle and a propulsion stage to a circular Low Earth Orbit (LEO) on one launch vehicle, launching the habitat module with another propulsion stage on a second launch vehicle to the same LEO, and then carrying out a single rendezvous and docking sequence to assemble the complete spacecraft stack. If more than two launches are required then the assembly sequence quickly becomes much more costly and complicated, and the probability of mission success drops accordingly.[2]

Various concepts have been proposed, ranging from the aforementioned assembly in LEO to crew rendezvous with pre-deployed resources at an Earth-Moon Lagrangian point prior to TNI. The NHATS elected to adopt the most straightforward option, which is departure from LEO. We currently have no experience with rendezvous, proximity operations, and docking in any orbit besides LEO*, and we currently have no in-

*The only exception to this is rendezvous in a circular Low Lunar Orbit (LLO) during the Apollo missions, but that orbital regime does not differ significantly from LEO for the purposes of spacecraft rendezvous, apart from slower dynamics (orbit rate comparable to that of Geosynchronous orbit).

frastructure in place to support the staging of equipment or propellant in a Lagrangian point orbit. In general, considerable non-existent infrastructure is required to make Earth departure from novel/exotic orbits practical for a NEO mission. By contrast, the only non-existent infrastructure item required to make departure from LEO practical is a heavy lift launch vehicle capable of delivering at least 100 t to LEO per launch. A heavy lift launch capability is important due to the high cost of launch vehicles and the safety/reliability penalty associated with using multiple launches to assemble the spacecraft prior to TNI. In fact, computing the IMLEO for a particular NEO mission opportunity, and from that deriving the required number of launches, provides a good metric for the quality, affordability, and attractiveness of a mission opportunity, where a smaller number of launches is better.

Modeling the TNI maneuver as being performed in LEO provides a conservative Δv calculation since other orbits can require less TNI Δv to achieve the same Earth departure C_3. For instance, the TNI Δv required at perigee on a highly elliptical orbit, such as a Geosynchronous Transfer Orbit (GTO), would be less than that required in LEO, all else being equal. Of course, a launch vehicle's capacity to deliver mass to a GTO is greatly reduced compared to the mass that can be delivered to LEO, so the overall advantage of performing TNI in a high energy orbit is unclear and depends on more than mass and Δv considerations. As an example, the Δv required to achieve a C_3 of 24 km^2/s^2 from a 400 km circular LEO is 4.232 km/s, whereas the Δv is only 1.902 km/s if performed at perigee on a typical GTO. However, to complete the example, the mass to LEO for an Atlas V 551 launch vehicle is approximately 18.8 t, whereas its approximate mass to GTO is only 8.9 t.

Thus, for the purposes of the NHATS, the Earth departure (TNI) maneuver is computed according to

$$\Delta v_{\text{TNI}} = \sqrt{C_3 + \frac{2\mu_{\text{E}}}{r_{\text{EPO}}}} - \sqrt{\frac{\mu_{\text{E}}}{r_{\text{EPO}}}} \tag{1}$$

where C_3 is the characteristic energy required for the particular mission opportunity, μ_{E} is Earth's gravitational parameter (3.986004415×10^5 km^3/s^2), and r_{EPO} is the radius of the circular Earth Parking Orbit (EPO)*. The NHATS assumes a 400 km altitude for the EPO, yielding a value for r_{EPO} of 6778.136 km (with an assumed Earth radius of 6378.136 km).

Another factor that can significantly impact the Earth departure phase of the mission is the asymptotic declination angle associated with the departure hyperbola. The inclination of the EPO should ideally be the same as the asymptotic declination angle, but the latitude of the launch site, along with restrictions on launch azimuth imposed for safety reasons (these vary between launch sites and among launch vehicles), will limit the EPO inclinations achievable from a particular launch site. The general result is that, as the absolute value of the asymptotic declination angle grows to exceed the magnitude of the launch site latitude, the mass that the launch vehicle can deliver to the EPO is reduced. If the asymptotic declination angle requires an EPO inclination that the launch site simply cannot provide due to the combination of launch site latitude and azimuth restrictions, then an achievable inclination for the EPO must be selected and additional Earth departure maneuvers must be performed to make up for the difference between EPO inclination and asymptotic declination angle. Reduced mass delivered to an EPO inclination that is achievable from the launch site chiefly impacts the required number of launches and is therefore not part of the NHATS calculations. The Δv penalty arising from an unachievable EPO inclination is best evaluated on a specific case-by-case basis and is therefore relegated to a post-processing step when necessary as it is beyond the scope of the NHATS analysis.

Earth Return

The NHATS assumes a direct atmospheric re-entry for the crew upon Earth return; that is, the crew vehicle arrives at Earth's Sphere of Influence (SOI) with some hyperbolic excess velocity, v_∞, and proceeds to

*Note that for departure from an elliptical orbit, the $\sqrt{\mu_{\text{E}}/r_{\text{EPO}}}$ term in Eq. (1) can simply be replaced with the velocity from the Vis-Viva or 2-body energy integral.

directly re-enter Earth's atmosphere when the incoming hyperbolic trajectory crosses Earth's effective atmospheric entry interface altitude. Thus the key consideration for this mission phase is the magnitude of the spacecraft's inertial velocity with respect to Earth at the effective atmospheric entry interface altitude. This velocity magnitude must be no greater than that which can be tolerated by the spacecraft's heat shield. For NHATS Phase I a maximum entry velocity magnitude of 12.5 km/s is assumed, and this threshold is reduced to 12.0 km/s for the Phase II analysis. For reference, the fastest re-entry velocity experienced by humans was 11.069 km/s during Apollo 10,[3] and in 2006 the fastest un-crewed Earth re-entry was performed by the Stardust Sample Return Capsule* at 12.9 km/s.

The velocity at Earth's entry interface, v_{EI}, depends on the incoming v_∞ and the radius of the entry interface, r_{EI}, according to

$$v_{\text{EI}} = \sqrt{v_\infty^2 + \frac{2\mu_{\text{E}}}{r_{\text{EI}}}} \tag{2}$$

where r_{EI} is equal to 6503.136 km (corresponding to an effective atmospheric entry interface altitude of 125 km). If the natural incoming v_∞ of the spacecraft produces a v_{EI} greater than the specified maximum, then the spacecraft must perform a maneuver that reduces v_{EI} to make it equal to the specified maximum. During NHATS Phase I, this maneuver is assumed to occur at the atmospheric entry interface and so is simply equal to the difference between the natural and maximum allowable v_{EI}. After further consideration we determined that it would be operationally infeasible to perform such a critical maneuver shortly before atmospheric entry. A better option is to perform the maneuver much farther from Earth, at Earth's SOI boundary. Thus in Phase II the maximum allowable v_{EI} is converted to the equivalent incoming v_∞ (by solving Eq. (2) for v_∞) and a maneuver at Earth's SOI to control v_∞ is modeled as

$$\Delta v_{\text{RET}} = v_\infty - v_{\infty_{\text{max}}} \tag{3}$$

Apart from being more operationally sound, physics dictates that this entry speed control strategy will require more Δv than performing the control maneuver at or near r_{EI} and thus it provides a more conservative value for the required Δv. Application of additional small maneuvers at certain points along the trajectory prior to Earth return can ensure that the spacecraft re-enters at favorable angles and within desirable latitude/longitude windows. That analysis is considered to be a post-processing step for NHATS, and will be applied to specific mission opportunities of interest rather than globally across all possible trajectory solutions.

While the direct entry strategy for Earth return is straightforward and has been successfully demonstrated during the Apollo missions, there are potential drawbacks. For instance, there is no way to salvage the crew's habitat module (e.g., transfer it into a parking orbit for later reuse), unless an additional propulsion module for that purpose is included in the vehicle design. Capturing into any kind of Earth orbit from an incoming hyperbolic trajectory requires substantial Δv and so carrying along the necessary propellant to perform such a maneuver for the habitat module would substantially increase the mission's required IMLEO. Thus an aerocapture for the habitat module (possibly using a ballute to augment the habitat module's ballistic coefficient) would be preferable when possible. However, aerocapture is unlikely to be practical for the crew vehicle, and it would be very difficult to provide the crew vehicle with sufficient propellant to insert itself into some sort of Earth-captured orbit upon return. Nevertheless, the ability to do so would be highly desirable if, for example, the crew vehicle's heat shield was damaged somehow during NEO proximity operations. In that case it would be necessary for the crew to insert into some sort of Earth orbit upon return so that they could be rescued since their heat shield would no longer be capable of withstanding atmospheric re-entry.

Optimal Circular Orbit Capture The goals of reusing the habitat module and providing a rescue option for the crew are certainly worthwhile, but the cost in terms of Δv (and therefore IMLEO) may be prohibitive for most NEO mission scenarios; pre-emplaced propellant at the NEO, or *in situ* resource utilization (ISRU) derived from the NEO, are examples of scenarios which would mitigate the effects on IMLEO. The significance of the Earth return capture cost can be readily understood by examining the Δv required to capture into

*http://en.wikipedia.org/wiki/Stardust_(spacecraft)

Earth orbit from an incoming hyperbola. Consider Eq. (1), which specifies the Δv necessary to perform TNI from the EPO. The same equation specifies the Δv necessary to capture into a circular orbit at a particular radius from an incoming hyperbola if we substitute the square of the incoming hyperbolic excess velocity, v_∞^2, for the Earth departure C_3 and substitute the desired capture orbit radius, r_{CAP}, for the departure parking orbit radius (r_{EPO}). The capture Δv is therefore determined by v_∞ and r_{CAP}. For a given v_∞ we can compute the value of r_{CAP} that minimizes the capture Δv by evaluating the derivative of the Δv equation with respect to r_{CAP}, equating the derivative to zero, and solving for the value of r_{CAP} that satisfies the equation.[4] This yields the capture orbit radius which minimizes capture Δv as

$$r_{\text{CAP}} = \frac{2\mu_{\text{E}}}{v_\infty^2} \tag{4}$$

If the capture orbit radius given by Eq. (4) is used, then the corresponding minimized capture Δv is

$$\Delta v_{\text{CAP}} = \frac{v_\infty}{\sqrt{2}} \tag{5}$$

For the set of minimum total Δv and minimum duration trajectory solutions generated during NHATS Phase II, the minimum *natural* (no control maneuver applied) Earth return v_∞ is 0.528 km/s, the mean is 4.443 km/s ($\sigma = 1.034$ km/s), and the maximum is 8.034 km/s. Most values of v_∞ for NEO missions will therefore lie between 3 and 5 km/s, but for completeness we will allow v_∞ to vary between 0.528 and 8.034 km/s in the brief analysis that follows. Table 1 presents particular optimal circular orbit capture solutions for various values of v_∞, including 4.627 km/s, which corresponds to the NHATS Phase II maximum allowable v_{EI} of 12.0 km/s.

Table 1. Selected Minimum Δv Solutions for Capture Into Circular Earth Orbit

Incoming v_∞, km/s	Optimal Capture Altitude, km	Capture Δv, km/s
0.528	2,853,187	0.373
3.000	82,200	2.121
4.627	30,858	3.272
5.000	25,510	3.536
8.034	5,973	5.681

Figures 2(a) and 2(b) show circular capture orbit altitude and associated minimum capture Δv, respectively, as a function of incoming v_∞. In Figure 2(a) it is clear that the minimum Δv circular capture orbit altitude increases to approximately 1 lunar distance from Earth as v_∞ decreases to approximately 1.4 km/s and quickly becomes much larger for $v_\infty < 1.4$ km/s; for $v_\infty < 0.925$ km/s, the minimum Δv capture orbit altitude actually exceeds Earth's SOI. Capturing into an orbit at greater than lunar distance does not seem practical operationally, and so from that standpoint the *practical* minimum capture Δv for a circular orbit will always be at least 1 km/s.

Furthermore, the incoming v_∞ will generally be greater than 1.4 km/s, most likely in the range of 3 to 5 km/s. Table 1 shows that the optimal capture orbit altitudes for v_∞ of 3 and 5 km/s are 82,200 and 25,510 km, respectively. These are rather large but not necessarily unreasonable. However, the associated capture Δv of 2.121 to 3.536 km/s is significant, considering that total mission Δv for most reasonable NEO mission designs ranges from approximately 4 to 7 km/s. An increase in Δv of 2 to 3.5 km/s to facilitate circular orbit capture at Earth return would dramatically increase the required IMLEO.

Elliptical Orbit Capture One possibility for reducing the necessary capture Δv is to capture into an elliptical orbit. This is an intuitive result considering that the spacecraft begins on a hyperbola with respect to Earth (escaped) and minimizing capture Δv therefore means reducing the spacecraft's energy only as much as necessary for an effective capture. Repeating the foregoing analysis with an elliptical capture orbit will show that there is no true minimum capture Δv associated with a given incoming v_∞, but that capture Δv

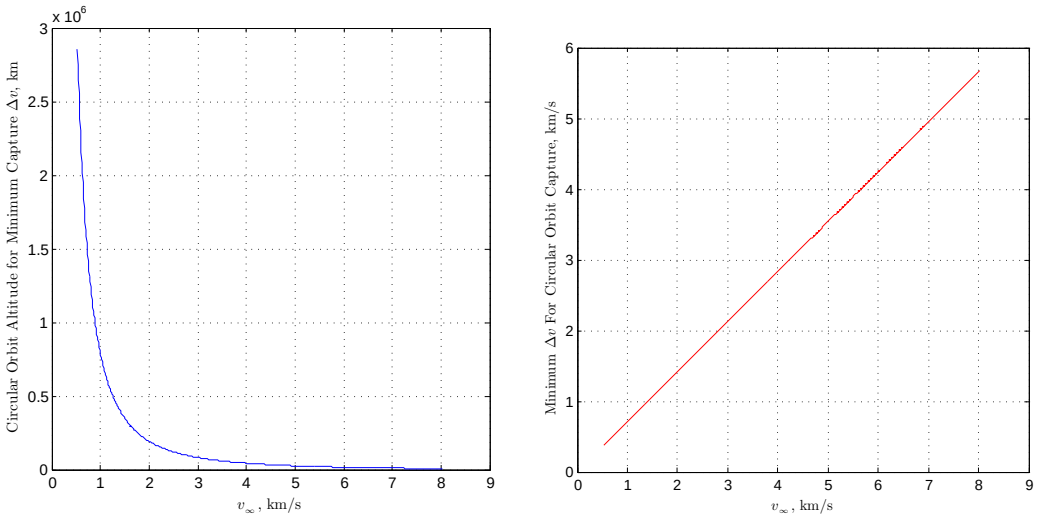

(a) Optimal Altitude for Circular Orbit Capture

(b) Minimum Δv for Circular Orbit Capture

Figure 2. Altitude and Corresponding Δv for Optimal Circular Orbit Capture as a Function of Incoming v_∞

decreases as the perigee of the elliptical capture orbit decreases and as the eccentricity of the capture orbit increases.

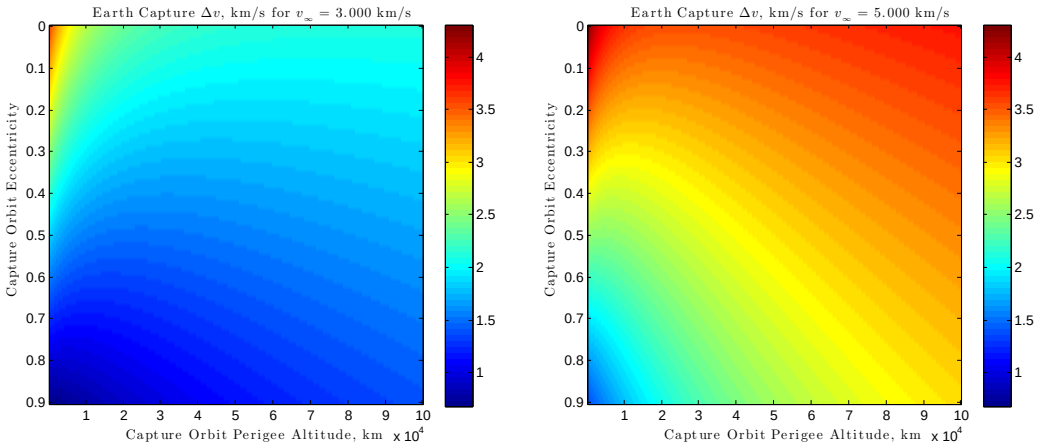

(a) Elliptical Orbit Capture Δv for v_∞ = 3 km/s

(b) Elliptical Orbit Capture Δv for v_∞ = 5 km/s

Figure 3. Elliptical Orbit Capture Δv for v_∞ of 3 and 5 km/s

Figures 3(a) and 3(b) present the required Δv to capture into elliptical orbits for v_∞ of 3 and 5 km/s, respectively. In each case the perigee altitude varies between 200 and 100,000 km and the eccentricity varies between 0 and 0.9. These figures show that the capture orbit must be rather eccentric (generally an eccentricity of 0.4 or greater) to yield any substantial capture Δv savings compared to optimal circular orbit captures at similar altitudes. The figures also illustrate the aforementioned behavior of the capture Δv (decreasing with decreasing elliptical capture orbit perigee and increasing eccentricity). Even with a perigee altitude of 200 km and an eccentricity of 0.9, the capture Δv is 0.680 km/s for a v_∞ of 3 km/s, and 1.361 km/s for a v_∞ of 5 km/s.

Thus even for an impractically eccentric capture orbit and minimal capture perigee, the capture Δv remains formidable. It is worth noting that crew rescue on a significantly elliptical orbit could be complicated by our lack of contemporary experience with rendezvous, proximity operations, and docking on elliptical orbits of any kind (much less extremely eccentric orbits). The only historical example of this sort of scenario occurred during Apollo lunar missions, during which CSM/LM transposition and docking was routinely performed post-TLI in a geocentric ellipse whose eccentricity exceeded 0.9.

Incoming Asymptotic Declination Angle Finally, note that the spacecraft will have some natural incoming asymptotic declination angle which will dictate the plane of the capture orbit (whether circular or elliptical) unless additional maneuvers are performed to adjust the plane, and that Δv would be in addition to the already formidable capture Δv discussed previously. The natural incoming asymptotic declination angle also constrains the latitudes and headings at which the spacecraft can re-enter Earth's atmosphere during a direct re-entry, and so some control of this angle may be necessary for logistical reasons even if no orbit capture is performed.

ANALYSIS METHODOLOGY

The objective of the NHATS is to identify all known NEAs which offer trajectory solutions within a given trajectory performance envelope and which also meet some minimum estimated size constraint. The fundamental process by which this analysis is performed was developed between November of 2009 and March of 2010, documented during the Summer of 2010 in Reference 1, and modified for the purposes of the NHATS during September of 2010. The primary difference between the pre-NHATS algorithm documented in Reference 1 and the NHATS version presented herein is that the pre-NHATS version of the algorithm includes notional launch vehicle and crew vehicle performance parameters used to filter out trajectory solutions which could not be flown under those vehicle performance constraints. That algorithm is modified for NHATS by removing the vehicle performance parameters and instead filtering trajectory solutions according to a trajectory performance envelope chiefly characterized by total mission Δv, mission duration, and Earth departure date. This permits a much broader assessment of the potential HSF accessibility of the known NEA population and allows all vehicle performance constraints to be applied in post-processing. A large database of trajectory solutions is thereby produced which can then be used repeatedly to perform a series of trade studies on mission architecture, vehicle performance, and launch requirements. In that way, the modified algorithm for the NHATS is more general and versatile.

One of the key findings from the studies presented in Reference 1 is that there is no simple way to determine whether a particular NEA will offer trajectory solutions within a given trajectory performance envelope, much less what the exact values of the trajectory solutions, if any, will be. For instance, there are no formulae operating on a NEA's heliocentric osculating orbital elements which will provide such an assessment. The only option is therefore to compute all of the possible round-trip trajectory solutions for the NEA in an efficient, organized manner. Reference 1 develops the necessary theory and framework for accomplishing this, facilitated by algorithms which require no propagation of Earth/NEA ephemeris or spacecraft trajectories and which readily admit to trivially parallelized distributed computing.

The core of the NHATS algorithm is based upon the method of embedded trajectory grids, illustrated in Figure 4. This method is described in detail in Reference 1 and constitutes an extension of the usual method by which so-called Pork Chop Contour (PCC) plots are generated for one-way trajectory opportunities between two orbit ephemerides (e.g., to simply travel from Earth to an asteroid, or from Earth to Mars. In those analyses, Lambert's problem is solved for every combination of departure date and Time of Flight (TOF) to yield the total Δv required to fly each possible one-way trajectory. The result is a grid of Δv values forming contours in the departure date vs. TOF space that allow all feasible trajectory opportunities to be identified (including the optimal solution(s)), and the "launch windows" or available departure seasons for the mission, which tend to repeat according to the synodic period between the departure and destination orbits.

Performing this sort of assessment for round-trip missions dramatically increases the complexity of the problem, as shown in Figure 4, because now the amount of time spent at the destination must be allowed to vary, along with the TOF to return to the starting location (e.g., Earth) on the initial departure orbit.

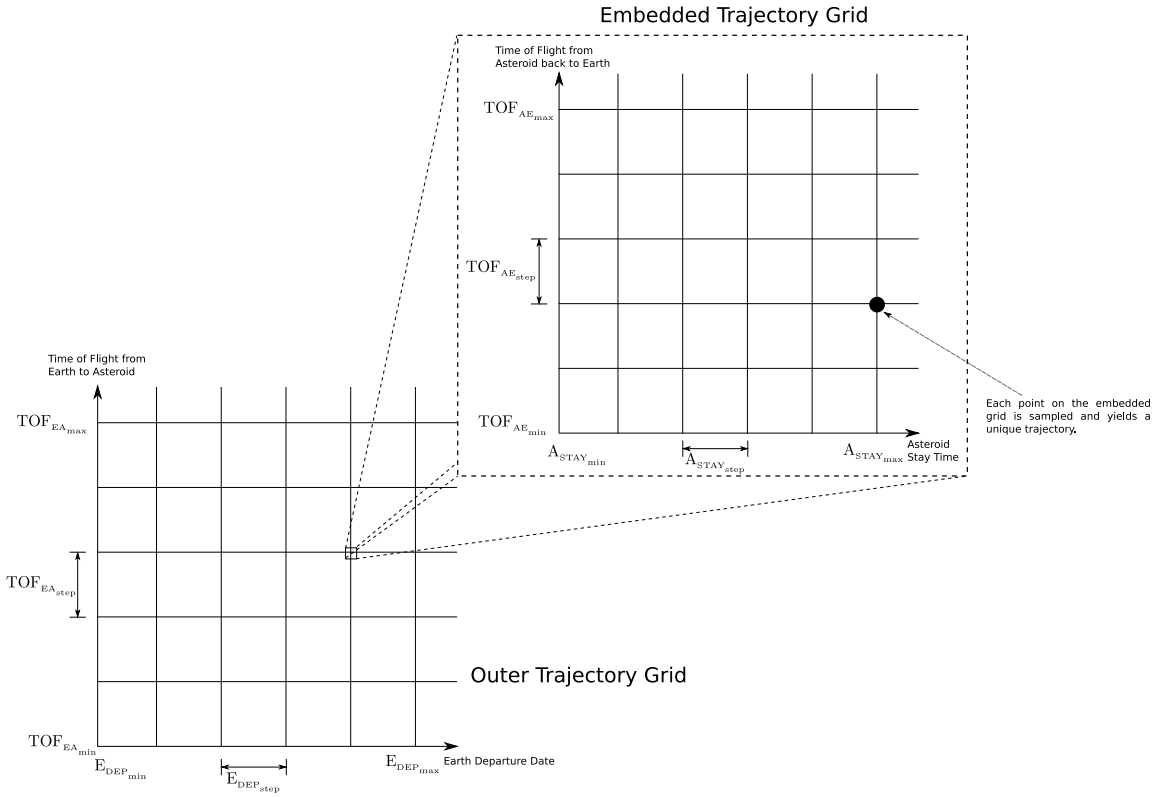

Figure 4. Embedded Trajectory Grids

Thoroughly assessing all the combinations of departure date, outbound TOF, stay time, and inbound TOF requires that secondary trajectory scan grids be "embedded" at every point on the traditional "outer grid" (which parametrizes only the outbound trajectory segment). Doing so causes a geometric increase in the total number of grid points that must be evaluated; furthermore, Lambert's problem must be solved *twice* (once for the outbound trajectory, and again for the inbound trajectory) for each of those grid points. In this context a "grid point" is defined as a particular set of values for (Earth departure date, outbound TOF, stay time, inbound TOF). Eq. (6) yields the total number of grid points, N, present within an embedded grid structure.

$$N = \left(\frac{\mathrm{E_{DEP_{max}} - E_{DEP_{min}}}}{\mathrm{E_{DEP_{step}}}} + 1\right) \times \left(\frac{\mathrm{TOF_{EA_{max}} - TOF_{EA_{min}}}}{\mathrm{TOF_{EA_{step}}}} + 1\right) \times \left(\frac{\mathrm{A_{STAY_{max}} - A_{STAY_{min}}}}{\mathrm{A_{STAY_{step}}}} + 1\right) \times \left(\frac{\mathrm{TOF_{AE_{max}} - TOF_{AE_{min}}}}{\mathrm{TOF_{AE_{step}}}} + 1\right) \tag{6}$$

The parameters in Eq. (6) are defined visually in Figure 4 and specify the boundaries and step sizes for the embedded grid structure.

Further constraints must still be applied to determine the actual value of N for a given case. First, only grid points which meet the total mission duration constraint are admissible, as specified in Eq. (7)

$$\mathrm{TOF_{EA}} + \mathrm{A_{STAY}} + \mathrm{TOF_{AE}} \leq \mathrm{TOF_{TOT_{max}}} \tag{7}$$

Secondly, the algorithm will stop in the outer grid whenever the maximum Earth departure C_3 constraint is violated; the number of grid points that will be excluded due to that is therefore unpredictable. Nevertheless, Eq. (6) subject to the Eq. (7) constraint provides a reasonable working estimate for N. Perhaps more importantly, it provides a good *relative* measure of N between different embedded grid parameter sets. A closed form solution for N, i.e., a single equation that incorporates the Eq. (7) constraint into Eq. (6), has not yet

been obtained and may not be obtainable. In the meantime, it is straightforward to write a simple computer program that counts to N using nested loops, with Eq. (7) enforced.

If the maximum Earth departure C_3 constraint is satisfied in the outer grid, the algorithm proceeds to evaluate the associated embedded grid. The total mission Δv for each combination of grid points is computed as the sum of the Earth departure Δv, the NEA arrival Δv, the NEA departure Δv, and the re-entry speed control Δv necessary upon Earth return, if any. Trajectory solutions for which the total mission Δv is less than or equal to the specified maximum value are then stored in an output data file; individual output data files are generated for each NEA that offers at least one trajectory solution that satisfies all constraints. Note that once N has been determined, it must be multiplied by the number of NEAs to be processed to yield the approximate number of grid points that will be processed in total.

STUDY CONSTRAINTS

The Phase I and Phase II iterations of the NHATS both utilized purposely inclusive trajectory filter constraints. This is motivated by the desire to obtain a broad view of the accessibility landscape and understand the correlations between trajectory performance envelopes (chiefly characterized by total mission duration, total mission Δv, and Earth departure date) and the numbers of NEAs offering trajectory solutions within those performance envelopes. *Due to the highly inclusive nature of the trajectory filter constraints, it is important to stress that passing the trajectory filter does not necessarily make a NEO accessible for HSF.*

Constraints Common to Phases I and II

Most of the constraints utilized in Phase I are modified in Phase II, but several constraints are left the same in both phases and are presented in Table 2. The constraints that change between the Phase I and Phase II studies are presented and compared in Table 3. The comparison and commentary in Table 3 make it clear that Phase II is intended to be even more inclusive than Phase I, while treating the atmospheric re-entry speed aspect of the problem more conservatively.

Table 2. Common NHATS Constraints for Phases I and II

Parameter	Value
Earth Departure Date	01/012015-12/31/2040
Total Mission Δv (km/s)	≤ 12.0
EPO Altitude (km)	400.0

Table 3. Differing NHATS Constraints for Phases I and II

Parameter	Phase I	Phase II	Phase II More/Less Inclusive?
SBDB Polling Date/Time	09/01/2010, 00:00 UTC	02/03/2011, 13:19 EST	More Inclusive
Earth Departure C_3 (km^2/s^2)	≤ 24	≤ 60	More Inclusive
Atmospheric Re-entry Speed (km/s)	≤ 12.5	≤ 12.0	Less Inclusive
Atmospheric Entry Interface Altitude (km)	121.92	125.0	Minor Change
Re-entry Speed Control Maneuver	$v_{\text{EI}} - v_{\text{EI}_{\max}}$	$v_\infty - v_{\infty_{\max}}$	Less Inclusive
Trajectory Grid Step Size (days)	6 (2 for stay time)	8 for all	Likely about the same
Minimum Outbound/Inbound TOF (days)	4	1	More Inclusive
Maximum Stay Time at NEA (days)	40	Unconstrained	More Inclusive
Maximum Mission Duration (days)	365	450	More Inclusive
Minimum Max. Estimated Size (m)	50	30	More Inclusive

The increase of the trajectory grid step sizes from 6 days to 8 days in Phase II is motivated by a desire to keep the total number of grid points per NEA, N, (as determined by Eq. (6) subject to Eq. (7), evaluated via a simple counting program) approximately the same as (but no greater than) it is in Phase I*. This necessitates a grid step size change because the maximum Phase II mission duration is increased to 450 days and the maximum NEA stay time constraint is removed. Note that while the NEA stay time is not explicitly constrained

*This will be a non-issue in future study iterations when larger computing clusters are utilized.

in Phase II, the total mission duration constraint is always in effect. The value of N for Phase I is 4.30×10^7, and the value of N for Phase II turns out to be 3.67×10^7 with the 8 day step size for the embedded grids.

The relationship between absolute magnitude, H, estimated NEO diameter, D (in km), and geometric albedo, p, is given by[5]

$$D = \frac{1329}{\sqrt{p}} 10^{-0.2H} \tag{8}$$

Eq. (8) is solved for H to convert the minimum estimated size constraints in Table 3 to H values. The reason that the estimated size constraint is couched as a "maximum" estimated size constraint in Table 3 is that a notional lower limit for NEA albedo of 0.05 is used when converting between diameter and H. Thus the size value computed for a given H is about as large as we would expect it to be; we are therefore being optimistic about the NEA's size (the NEA might actually have a higher albedo and thus would have a smaller diameter for a given H). This yields an absolute magnitude criterion in Phase I of $H \leq 25.37$; for Phase II the criterion is $H \leq 26.5$.

RESULTS

Phase I

In Phase I the 7,116 NEAs within the SBDB as of 09/01/2010, 00:00 UTC were processed in 6 hours using 158 CPU cores. 666 of those NEAs offer at least one NHATS-qualifying trajectory solution, and the total number of NHATS-qualifying trajectory solutions was 82,691,955. 433 of those 666 NEAs also meet the constraint of estimated size $\geq$ 50 m ($H \leq 25.37$). The total number of unique trajectory solutions for those 433 NEAs is 34,021,464.

The minimum, mean, and maximum of the absolute magnitudes of the 433 Phase I NHATS-qualifying NEAs are 15.750, 22.867, and 25.366, respectively. These correspond to maximum, mean, and minimum estimated sizes (at p = 0.05) of 4207.654, 254.446, and 50.216 m, respectively. The minimum total mission duration found is 34 days, and the mean across all trajectory solutions is 232 days. The overall minimum total Δv found is 3.549 km/s, and the average minimum total Δv is 9.495 km/s. The minimum number of viable trajectory solutions found for a NEA is 1, the mean for all 433 NEAs is 78,571, and the maximum is 4,153,445.

The minimum, mean, and maximum values for semimajor axis, a, across the 433 NEAs are 0.770, 1.150, and 1.665 AU, respectively. For orbital eccentricity, e, the minimum, mean, and maximum values are 0.012, 0.224, and 0.444, respectively, and for orbital inclination, i, the minimum, mean, and maximum values are 0.111°, 6.194°, and 16.226°, respectively. In terms of NEA orbit classification, the 433 NHATS-qualifying NEAs consist of 115 Atens (26.56%), 234 Apollos (54.04%), and 84 Amors (19.40%). The definitions of these NEA orbit classifications are presented in Figure 5.

Phase II

In Phase II the 7,665 NEAs within the SBDB as of 02/03/2011, 13:19 EST were processed in 52 hours using 20 CPU cores. 765 of those NEAs offer at least one NHATS-qualifying trajectory solution, and the total number of NHATS-qualifying trajectory solutions is 79,157,604. 590 of those 765 NEAs also meet the constraint of estimated size $\geq$ 30 m ($H \leq 26.5$). The total number of unique trajectory solutions for those 590 NEAs is 39,428,709.

The minimum, mean, and maximum of the absolute magnitudes of the 590 Phase II NHATS-qualifying NEAs are 15.750, 23.459, and 26.468, respectively, and the distribution of H for the Phase II NHATS-qualifying NEAs is shown in Figure 6(a); the distribution of H is quite similar in Phase I. The statistics for H correspond to maximum, mean, and minimum estimated sizes (at p = 0.05) of 4207.654, 214.946, and 30.230 m, respectively, and the estimated size distribution is shown in Figure 6(b); again, the distribution for the Phase II results is quite similar to that for the Phase I results. The minimum total mission duration found is 34 days, and the mean across all trajectory solutions is 245 days. The overall minimum total Δv found

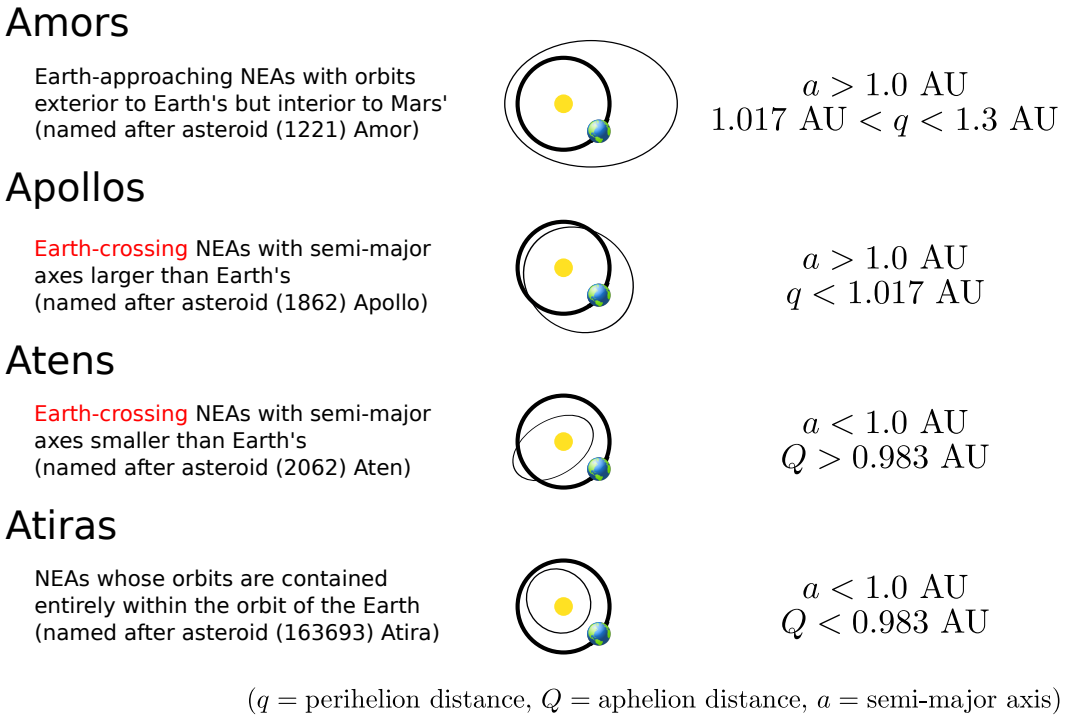

Figure 5. NEA Orbit Classifications

is 3.551 km/s, and the average minimum total Δv is 9.458 km/s. The minimum number of viable trajectory solutions found for a NEA is 1, the mean for all 590 NEAs is 66,828, and the maximum is 3,302,638.

The minimum, mean, and maximum values for semimajor axis, a, across the 590 NEAs are 0.770, 1.154, and 1.699 AU, respectively. For orbital eccentricity, e, the minimum, mean, and maximum values are 0.012, 0.228, and 0.417, respectively, and for orbital inclination, i, the minimum, mean, and maximum values are 0.021°, 5.726°, and 15.485°, respectively. In terms of NEA orbit type, the 590 NHATS-qualifying NEAs consist of 150 Atens (25.42%), 332 Apollos (56.27%), and 108 Amors (18.31%).

Considering the semilatus rectum values for the NEA orbits allows the semimajor axis, eccentricity, and inclination envelope of the NHATS-qualifying NEAs to be visualized on a single two-dimensional plot since the semilatus rectum is equal to $a\left(1-e^2\right)$. This plot is shown in Figure 7(a) and indicates that as inclination increases, the semilatus rectum must become closer to 1 AU (generally, more Earth-like) in order for the NEA to pass the NHATS trajectory filter. Figure 7(b) shows that as eccentricity increases, semimajor axis must become greater than or less than 1 AU to permit close approaches to Earth at NEA perihelion or aphelion, respectively. Likewise, as eccentricity decreases, semimajor axis must be closer to 1 AU to permit close approaches between the NEA and Earth. The trends shown in Figures 7(a) and 7(b) for the Phase II results are essentially the same as the trends associated with the Phase I data.

The top 25 NEAs, in terms of the number of viable trajectory solutions offered by each, are shown in Table 4. 48% of the top 25 NEAs are Atens, 36% are Apollos, and 16% are Amors. Table 4 presents two trajectory solutions for each NEA: the overall minimum duration solution and the overall minimum total round-trip Δv solution. The minimum and maximum estimated size values shown for each NEA in Table 4 are computed from Eq. 8 using the aforementioned values for p of 0.25 and 0.05, respectively.

Phase IIa

A follow-on to Phase II was performed on 05/28/2011 in order to update the NEA trajectory database while NHATS automation work continued. The SBDB contained 7,974 NEAs as of 05/28/2011, 00:34 EDT,

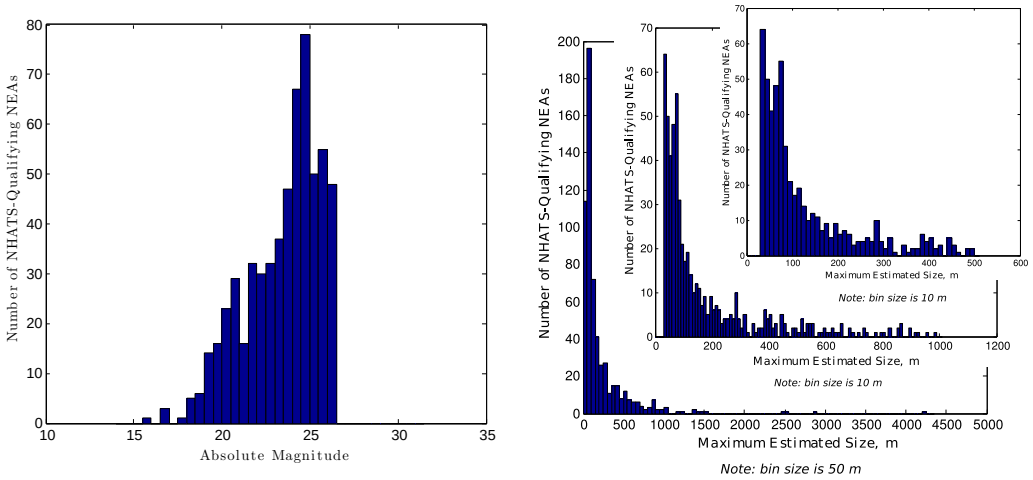

(a) Distribution of Absolute Magnitude (bin size is 0.5)

(b) Distribution of Maximum Estimated Size

Figure 6. Distributions of Absolute Magnitude and Maximum Estimated Size for the Phase II NHATS-Qualifying NEAs

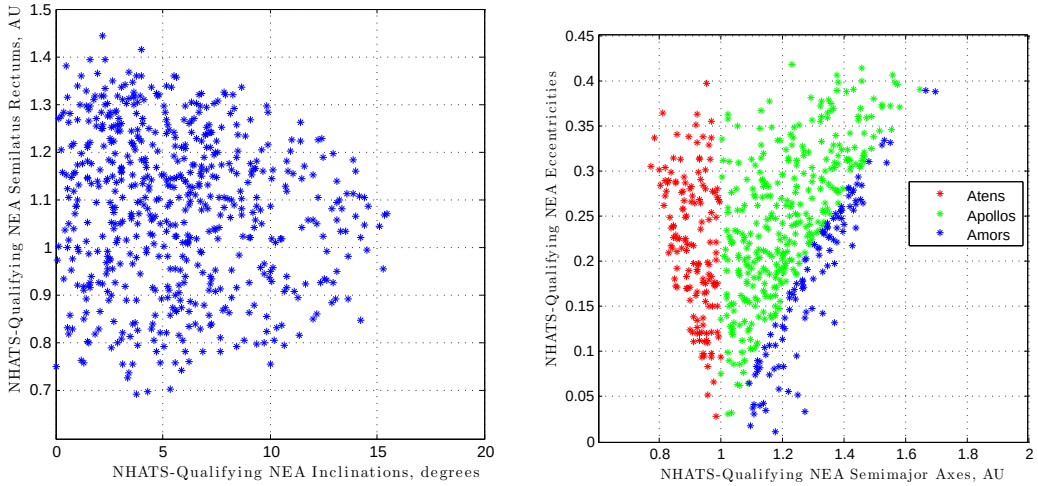

(a) Semilatus Rectum vs. Inclination

(b) Eccentricity vs. Semimajor Axis

Figure 7. Relationships Between Phase II NHATS-Qualifying NEA Orbital Elements

Table 4. Top 25 NEAs in NHATS Phase II, Ranked by Number of Viable Trajectory Solutions

Rank	Designation	# Viable Sol.	H	Est. Size (m)	Orbit Type	Min. TOF (days)	Δv (km/s)	Dep. Date	Min. Δv (km/s)	TOF (days)	Dep. Date
1	2000 SG_{344}	3,302,638	24.79	29 - 66	Aten	34	11.558	6 Apr. 2028	3.551	370	10 Oct. 2029
2	2006 BZ_{147}	1,674,416	25.43	22 - 49	Apollo	58	11.928	20 Jul. 2037	4.110	370	13 Feb. 2035
3	2001 FR_{85}	1,618,888	24.51	33 - 75	Aten	58	11.631	3 Aug. 2039	4.292	362	28 Sep. 2039
4	2010 UJ	1,082,350	26.18	15 - 34	Aten	50	11.821	26 Aug. 2033	4.376	450	27 Sep. 2033
5	2009 HE_{60}	970,582	25.67	20 - 44	Aten	210	11.998	9 Dec. 2016	6.962	442	15 Jul. 2035
6	2007 YF	791,134	24.77	30 - 66	Aten	58	11.929	8 Oct. 2034	5.431	346	25 Nov. 2034
7	2010 JK_1	773,964	24.42	35 - 78	Apollo	106	11.789	17 Sep. 2035	4.854	402	12 Apr. 2033
8	2004 VJ_1	679,319	24.27	37 - 83	Aten	122	11.749	20 Oct. 2015	6.034	450	14 May 2036
9	2009 YF	663,423	24.69	31 - 69	Aten	74	11.928	21 Sep. 2028	5.660	450	2 Dec. 2028
10	1993 HD	656,700	25.63	20 - 44	Amor	98	11.917	24 Feb. 2036	6.045	442	31 Jan. 2036
11	2001 QJ_{142}	638,089	23.42	55 - 123	Apollo	74	11.947	15 Feb. 2024	5.425	362	3 Oct. 2035
12	2006 FH_{36}	630,084	22.92	69 - 155	Aten	114	11.946	21 Jun. 2035	5.996	362	14 Mar. 2034
13	2009 HC	555,180	24.77	30 - 66	Apollo	66	11.752	7 Feb. 2027	4.430	362	17 Apr. 2026
14	2011 AA_{37}	546,096	22.78	74 - 165	Amor	122	11.895	12 Jun. 2026	5.835	386	20 Jun. 2026
15	1999 CG_9	541,015	25.23	24 - 53	Apollo	66	11.770	8 Dec. 2033	5.216	370	10 Aug. 2033
16	2007 UY_1	537,599	22.88	71 - 158	Aten	122	11.970	16 Dec. 2033	5.505	362	2 Mar. 2021
17	2005 QP_{11}	491,888	26.43	14 - 31	Aten	122	11.731	12 Jul. 2031	5.805	394	28 Feb. 2029
18	2009 OS_5	478,949	23.57	51 - 115	Amor	42	11.914	30 May 2036	6.072	410	15 Jun. 2036
19	2009 DB_{43}	477,581	26.46	14 - 30	Apollo	82	11.614	26 Aug. 2030	6.249	378	25 Aug. 2015
20	2001 CQ_{36}	473,574	22.70	77 - 171	Aten	162	11.943	25 Jan. 2031	5.826	354	30 Jun. 2021
21	2004 JN_1	465,681	23.45	54 - 121	Apollo	106	11.562	25 Oct. 2020	6.220	354	4 Jun. 2029
22	1999 AO_{10}	462,650	23.86	45 - 101	Aten	50	11.766	26 Dec. 2025	5.780	418	27 Jan. 2026
23	2003 SM_{84}	445,022	22.73	76 - 169	Amor	74	11.889	23 Apr. 2040	6.360	370	20 Sep. 2039
24	2009 CV	434,988	24.25	37 - 84	Apollo	50	11.891	27 Jan. 2029	5.709	322	9 Aug. 2015
25	2009 TP	433,374	23.54	52 - 117	Apollo	154	11.981	2 Aug. 2033	5.916	370	4 May 2035

an increase of 309 NEAs since the Phase II SBDB polling date. Since 114 days elapsed between the Phase II SBDB polling date of 02/03/2011 and the Phase IIa polling date of 05/28/2011, the *average* rate at which NEAs were added to the SBDB during that interval was approximately 2.7 NEAs per day, or approximately 80 NEAs per lunation.

These 309 NEAs were processed in 10.6 hours using 4 CPU cores. 63 of the NEAs passed the trajectory filter, yielding 3,605,931 trajectory solutions, and 49 of those also meet the minimum estimated size constraint, yielding 1,747,060 trajectory solutions. This raises the total number of NEAs which pass the Phase II trajectory filter to 828, and raises the total number of NEAs which pass the Phase II trajectory filter and also meet the Phase II minimum estimated size constraint to 639.

The minimum, mean, and maximum of the absolute magnitudes of the 49 Phase IIa NHATS-qualifying NEAs are 20.530, 24.452, and 26.450, respectively. These correspond to maximum, mean, and minimum estimated sizes (at p = 0.05) of 465.629, 107.470, and 30.482 m, respectively. The minimum total mission duration found is 66 days, and the mean across all trajectory solutions is 249 days. The overall minimum total Δv found is 5.916 km/s, and the average minimum total Δv is 9.780 km/s. The minimum number of viable trajectory solutions found for a NEA is 3, the mean for all 49 NEAs is 35,654, and the maximum is 230,661.

The minimum, mean, and maximum values for semimajor axis, a, across the 49 NEAs are 0.810, 1.144, and 1.670 AU, respectively. For orbital eccentricity, e, the minimum, mean, and maximum values are 0.050, 0.236, and 0.390, respectively, and for orbital inclination, i, the minimum, mean, and maximum values are 0.410°, 5.394°, and 13.920°, respectively. In terms of NEA orbit type, the 49 NHATS-qualifying NEAs consist of 14 Atens (28.57%), 25 Apollos (51.02%), and 10 Amors (20.41%).

Discussion

The number of NEAs added to the SBDB between Phase I and Phase II is 549, representing a 7.715% increase in the known NEA population. Since 155 days elapsed between the Phase I and Phase II SBDB polling times, the *average* NEA discovery rate over that interval was about 3.5 NEAs per day, or 104.6 NEAs per lunation; this is slightly higher than the average rate of 2.7 NEAs per day / 80 NEAs per lunation between Phase II and Phase IIa). Of the 549 NEAs discovered between Phases I and II, 97 (17.668% of the new discoveries) passed the Phase II trajectory filter, and of these, 62 (11.293% of the new discoveries) also met the minimum estimated size constraint ($H \leq 26.5$).

The higher discovery rate between Phase I and Phase II is attributable to the fact nearly all NEO surveys are performed in the Northern Hemisphere, which is in winter during the September 2010 - February 2011 interval. During winter the nights are longer, allowing more time for telescopes to identify faint NEOs.

Another effect which tends to increase the discovery rate during winter in the Northern Hemisphere is the fact that the ecliptic is high in the sky during the fall and winter months, and searches are optimized by searching both sides of the ecliptic. During summer months the ecliptic is much lower relative to the horizon and so it is more difficult for telescopes to provide coverage south of the ecliptic. Finally, NEO discoveries are also hampered during summer months because the ecliptic passes through galactic latitude of zero, presenting a more dense star background.*

The number of NEAs that pass the trajectory filter increases from 666 in Phase I to 765 in Phase II; the 99 additional NEAs represent a 14.865% increase. The number of NEAs that pass the trajectory filter *and* meet the minimum size constraint increases from 433 in Phase I to 590 in Phase II; the 157 additional NEAs represent a 36.259% increase. However, recall that only 97 of the NEAs discovered between Phases I and II pass the Phase II trajectory filter, and of those only 62 also meet the minimum estimated size constraint.

The differences in trajectory filter and minimum estimated size constraint must also be accounted for when comparing Phase I and II results. Of the 765 NEAs that pass the Phase II trajectory filter, 48 did not originally pass in Phase I. Also, 46 of the 666 NEAs from Phase I did not pass the trajectory filter in Phase II. Likewise, 128 of the 590 NHATS-qualifying NEAs found in Phase II are not among the 433 NHATS-qualifying NEAs identified in Phase I. Further, 33 of the 433 Phase I NEAs did not pass the trajectory and size filters in Phase II.

Thus, the increase in the number of qualifying NEAs in Phase II, as compared to Phase I, is not solely due to the increase in the known NEA population. The careful comparison outlined above demonstrates that changes in the trajectory filter parameters and, to a somewhat greater extent, the reduction in the minimum estimated size constraint (from 50 to 30 m) have an appreciable effect on the outcome. In terms of the total number of NHATS-qualifying NEAs, the net increase in Phase II from Phase I is due to the relaxation of the minimum estimated size constraint to 30 m, the net difference between the more and less inclusive trajectory filter parameters described in Table 3, and the increase in the known NEA population due to discoveries between 09/01/2010 and 02/03/2011.

Also of interest is the subtle change in the distribution of heliocentric osculating orbital elements for the 590 Phase II NHATS-qualifying NEAs as compared to the distribution found in the 433 Phase I NEAs. In particular, the Phase II trajectory filter selects slightly lower inclination NEAs than those found during Phase I. This is likely due to the combination of reduced maximum allowable atmospheric re-entry speed and the more conservative re-entry speed control maneuver calculation since those are the only constraints which become less inclusive in Phase II.

Table 4 presents the top 25 NEAs identified in NHATS Phase II, ranked in descending order of the number of viable trajectory solutions offered. While not a perfect metric for absolute accessibility (particularly in the absence of a well-defined mission architecture and vehicle elements), the number of viable trajectory solutions does provide a good measure of *relative* accessibility, correlates reasonably well with the availability of low Δv mission opportunities with reasonable durations, and is representative of Earth departure season duration. This can be seen by examining the PCC plots for the top 4 NEAs, shown in Figure 8.

Note that while 2000 SG_{344}, 2006 BZ_{147}, and 2010 UJ all offer at least some low Δv, low duration mission opportunities within the 2025 - 2035 time frame (with 2000 SG344 clearly offering the best accessibility season), the accessibility season offered by 2001 FR85 does not begin until shortly after 2035 and its best opportunities (which include some relatively low Δv mission opportunities with duration $\leq$ 180 days) do not occur until the late 2030s.

ADVANCED TRAJECTORY MODELING

The University of Maryland (UMD) and Arizona State University (ASU) collaborated during the Fall 2010 and Spring 2011 semesters to complete a senior design project dubbed the Manned Vehicle for Exploration and Research Into the Cosmos (MAVERIC). The goal of the project is to create a comprehensive design

*Abell, Paul (2011), personal correspondence of July 21st. Lead Scientist for Planetary Small Bodies, Astromaterials Research & Exploration Science Directorate, NASA Johnson Space Center, Houston, TX.

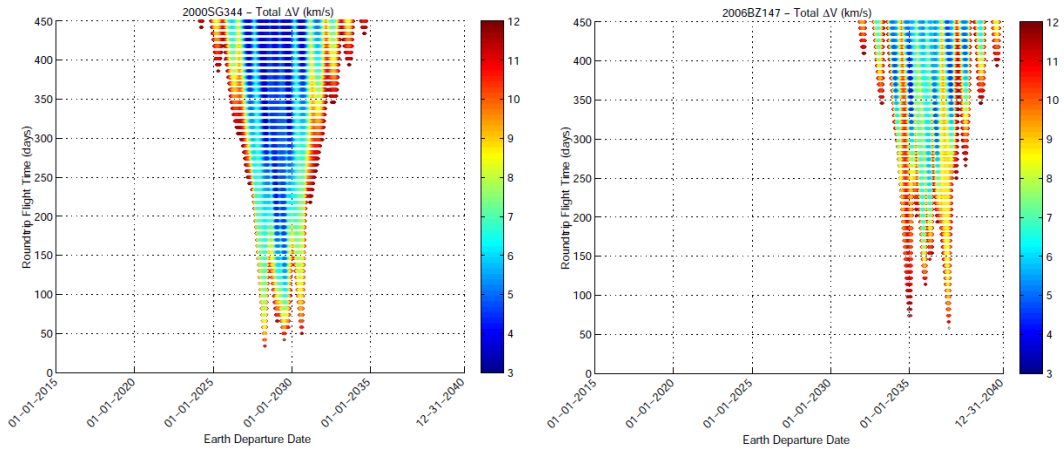

(a) PCC Plot for 2000 SG_{344}

(b) PCC Plot for 2006 BZ_{147}

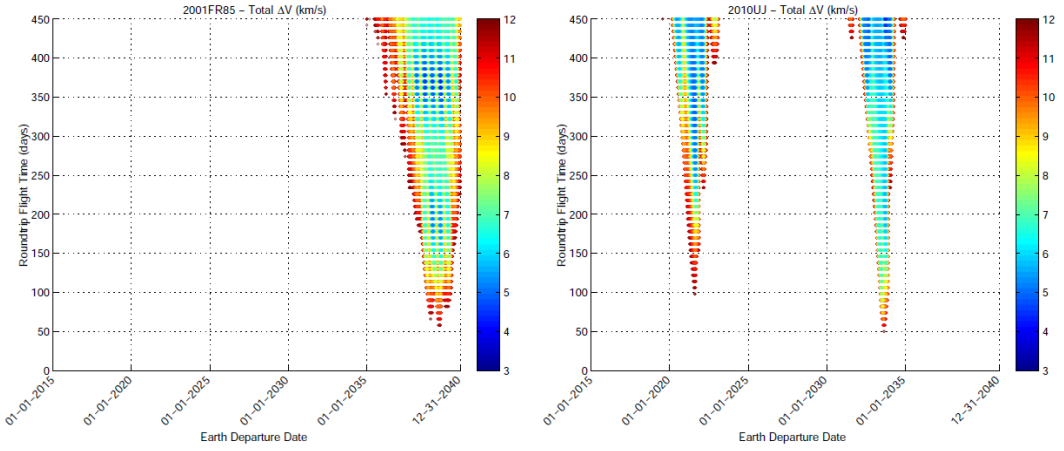

(c) PCC Plot for 2001 FR_{85}

(d) PCC Plot for 2010 UJ

Figure 8. PCC Plots for the Top 4 NEAs from Table 4

for a space program that includes multiple six-month HSF missions to NEAs which launch between 2020 and 2030, use current and near term technology, and carry robotic assistants called Exo-SPHERES. The Exo-SPHERES are fully autonomous robots built and designed by UMD to carry multiple science packages designed by ASU and assist the astronauts in exploring and characterizing the destination NEA. The spacecraft design also includes an inflatable structure called the X-Hab, which is an inflatable habitat attached to the service module of the MAVERIC vehicle. It provides the primary living quarters for the astronauts, protecting them from the deep space environment and providing sufficient habitable volume.

Previous NEA trajectory surveys are examined when deciding which NEA to visit, including the NHATS. The following NEAs are selected using NHATS data, based on estimated NEA diameter, available launch years, mission durations, and low Δv mission opportunities: 2007 XB_{23}, 2001 QJ_{142}, 1999 AO_{10}, and 2000 SG_{344}. The NHATS trajectory data show these four NEAs all offer low total Δv solutions (all < 7 km/s) with opportunities for missions with durations of approximately six months that launch between 2020 and 2030. PCC plots are then examined to find specific launch opportunities and the best trajectory solution for each asteroid is then located in the NHATS trajectory data files. The MAVERIC team has designed complete missions to all four NEAs, but for the sake of brevity we will only present results for 2000 $SG344_{344}$ as an example of the trajectory analysis performed for each NEA.

The trajectory analysis is performed using AGI's Satellite Tool Kit Version 9 (STK 9). Parameters are varied slightly in an effort to notionally optimize the trajectory solutions whilst respecting mission constraints and satisfying requirements. The Astrogator module in STK 9 is seeded with the parameters for the best trajectory solution found within the NHATS trajectory data file, including Earth departure date, EPO altitude, EPO inclination (to match departure asymptotic declination angle when possible), and flight times (outbound, NEA stay time, and inbound). Astrogator's differential corrector is then used with STK's built-in high-fidelity force models to converge on the notionally optimized trajectory solution for each NEA. The HSF NEA mission profile shown previously in Figure 1 serves as the primary model for the STK 9 scenario, and the resulting STK 9 heliocentric trajectory solution for a mission to 2000 $SG344_{344}$ is shown in Figure 9. Earth's orbit is rendered in green and 2000 $SG344_{344}$'s orbit is rendered in a teal color. The mission sequence begins with an Earth departure maneuver that places the spacecraft onto the outbound trajectory, rendered in red, which intercepts the NEA. An arrival maneuver to match NEA velocity is then performed as the spacecraft nears the NEA. The spacecraft remains in the vicinity of the NEA for a specified amount of time (rendered in blue), after which an NEA departure maneuver places the spacecraft onto an Earth return trajectory, rendered in yellow.

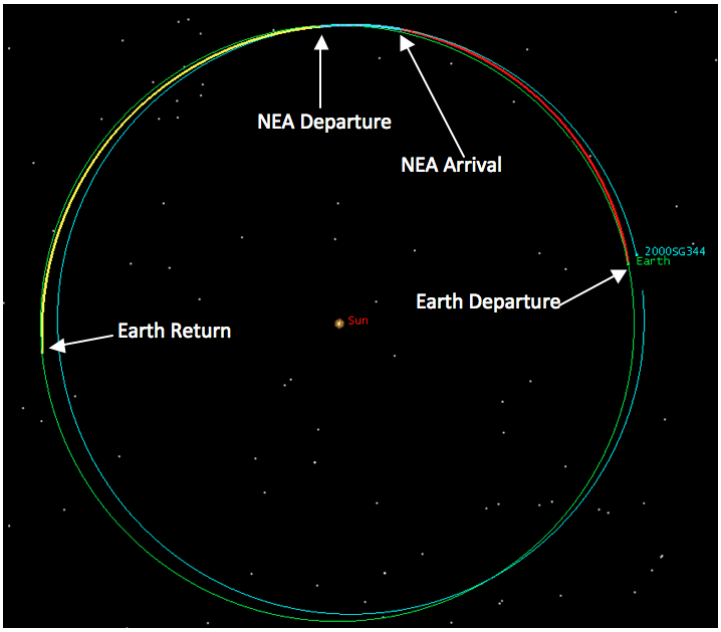

Figure 9. Round-Trip Trajectory Solution Generated with STK/Astrogator for 2000 SG_{344} Mission

Using STK 9 for the trajectory analysis is advantageous because the parameters for a notionally optimal solution identified on a PCC plot can be provided as input and then other mission/trajectory parameters can be easily varied as mission requirements change. The complete set of geocentric parameters for the EPO can also be determined, particularly Right Ascension of the Ascending Node (RAAN) and true anomaly necessary for Earth departure near the specified date/time. Note that the NHATS trajectory solution utilizes a reference value for circular EPO altitude and computes the necessary asymptotic declination angle for Earth departure. The asymptotic declination angle would ideally drive the EPO inclination, but this is impractical in some cases due to launch safety concerns. Here again Astrogator proves useful because the EPO inclination can be constrained whilst allowing Astrogator to vary the exact time of the Earth departure maneuver so as to correct for the inability of the EPO's inclination to match the specified asymptotic declination angle.

The outbound trajectory sequence is divided into the following segments: departure from the EPO, propagation to 100,000 km from Earth using the high-fidelity HPOP propagator, propagation to Earth's SOI (925,000 km from Earth) using the cislunar propagator, and propagation to arrival near the NEA using the heliocentric propagator. The spacecraft's stay time at the NEA is also propagated with the heliocentric propa-

gator, and the inbound trajectory sequence is constructed using the same segments as the outbound sequence, ending with Earth return at the 125 km atmospheric entry interface altitude. All heliocentric propagations included gravitational perturbations from the major solar system bodies. Note that only the spacecraft's motion is propagated; the NEA's ephemeris is supplied by a spice file downloaded from JPL HORIZONS, while STK internally uses DE405 ephemeris for all major solar system bodies.

Using STK 9 with NHATS data, the MAVERIC team has been able to determine how the total mission Δv is impacted by the combination of launch site constraints, EPO altitude, and asymptotic declination angle. These studies are very valuable because the NHATS assumes a 400 km altitude EPO and does not constrain EPO inclination. For the case of 2000 $SG344_{344}$, a launch from Kennedy Space Center (KSC) is assumed, from which launch azimuths are constrained so as to confine available EPO inclinations to be between 28.5° and 62°; these limits did not include any launch vehicle-specific constraints. The results for the 2000 $SG344_{344}$ case are presented in Table 5 and compared to the NHATS trajectory solution. Since the 2000 $SG344_{344}$ trajectory solution calls for an asymptotic declination angle of -22.066°, the minimum available inclination from KSC was used for the EPO and Astrogator was set to allow the exact time of the departure maneuver to vary so as to achieve the desired outbound trajectory.

A second validation of this trajectory solution was recently performed using the MacHILT (HILT = Heliospheric Interactive Lambert Targeting) precision trajectory design software. The MacHILT results are presented alongside the results from NHATS and STK 9 / Astrogator in Table 5, and a geocentric mission trajectory plot from MacHILT is presented in Figure 10. The close agreement of results between the NHATS software, STK 9, and MacHILT shown in Table 5 demonstrates the accuracy of the NHATS data and highlights the capability of both STK 9 / Astrogator and MacHILT to utilize NHATS data, in combination with realistic mission constraints, to produce fully integrated precision trajectory solutions for round-trip NEA missions.

While all three trajectory design solutions in Table 5 agree quite closely, it is important to note that both the STK 9 and MacHILT solutions are able to reduce the total Δv required for the mission by about 1% while essentially preserving the other design features to within $< 1\%$. Although this very small Δv reduction is unremarkable on its own, the fact that it is a reduction and not an increase demonstrates that the NHATS software is not underestimating the Δv requirements for NEA missions; rather, the NHATS software is inherently overestimating the Δv by a very, very small margin. This slight inherent conservatism is highly desirable in a broad trajectory survey tool.

Table 5. 2000 SG_{344} Trajectory Design Results Obtained from the NHATS, STK 9, and MacHILT

Parameter	NHATS	STK	MacHILT
Earth Departure Date & Time (UTCG)	6 Jul. 2029, 00:00	5 Jul. 2029, 23:26	5 Jul. 2029, 21:07
Earth Departure C_3 (km^2/s^2)	1.475	1.180	1.128
Δv to Depart Circular LEO (km/s)	3.244	3.229	3.224
Departure LEO Altitude (km)	400	400	400
Earth Departure Asymptotic Declination	-22.066°	-21.879°	-21.939°
Flight Time from Earth to NEA (days)	73	72.22	70.62
NEA Arrival Δv (km/s)	0.684	0.675	0.702
NEA Stay Time (days)	16	16	18.5
NEA Departure Δv (km/s)	0.814	0.767	0.777
Flight Time from NEA to Earth Return	89	88.652	89.416
Earth Return v_∞ (at SOI crossing) (km/s)	1.073	0.965	0.938
Earth Return Asymptotic Declination	19.773°	19.169°	19.128°
Atmospheric Re-entry Speed at 125 km Altitude (km/s)	11.124	11.114	11.112
Total Mission Δv (km/s)	**4.742**	**4.671**	**4.703**
Total Mission Duration (days)	**178.00**	**176.87**	**178.659**

CONCLUSION

The NHATS has identified hundreds of NEAs which pass a purposely inclusive trajectory filter, but only a handful of them may offer truly viable opportunities for HSF exploration between the mid-2020s and mid-2030s. The more important result is that the NHATS has established an efficient, comprehensive, and repeatable process by which the growing known NEA population may be systematically monitored for HSF

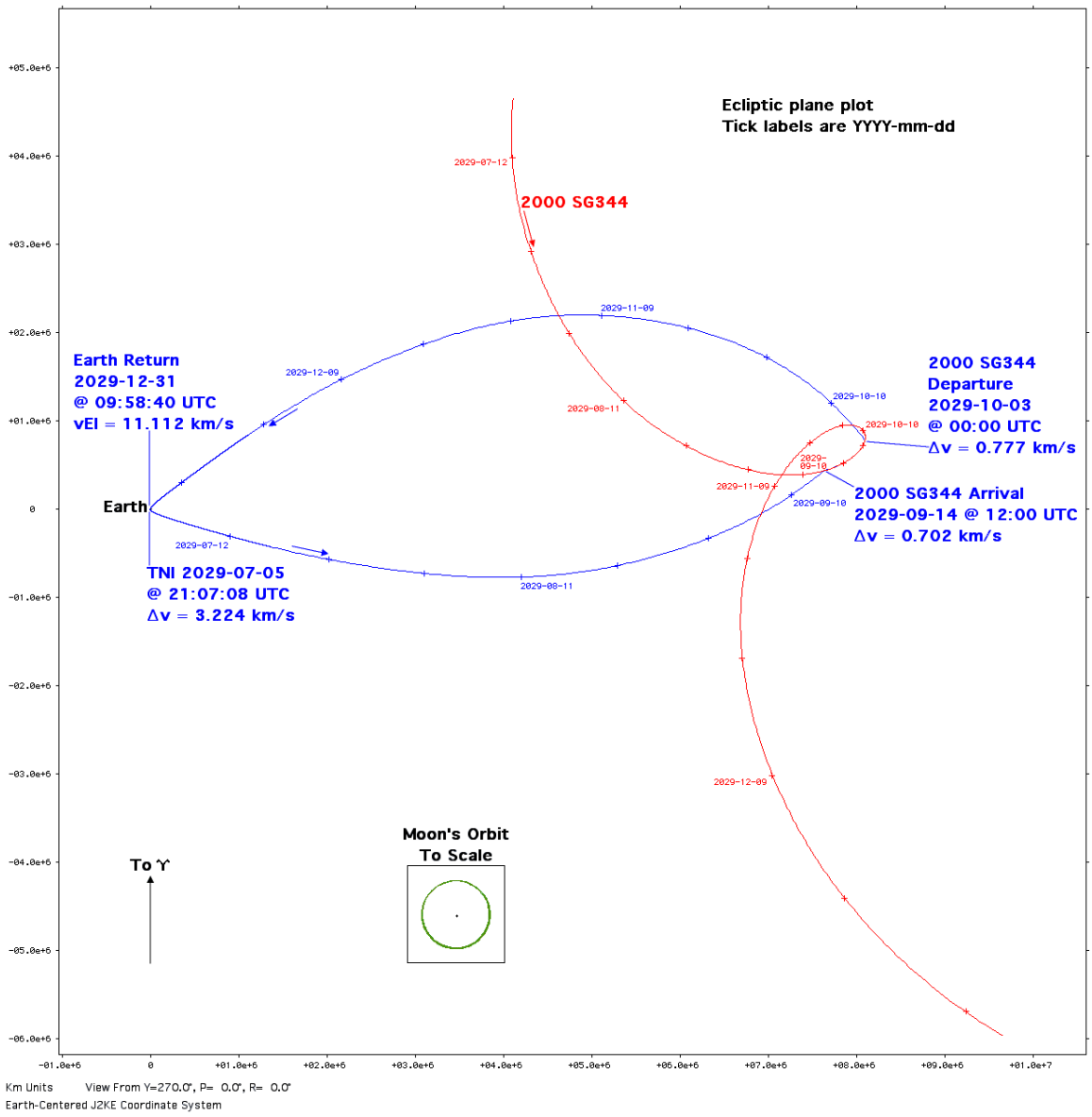

Figure 10. MacHILT Geocentric Precision Trajectory Design

accessibility as more and more NEAs are discovered, akin to the way in which JPL and the University of Pisa in Italy currently monitor the entire NEO population for Earth impact risk. As NASA's forward path gains clarity and momentum, and as the future of HSF architecture becomes defined, the NHATS will be keeping pace with NEA discoveries so that we find the best targets for our future explorers, human and robotic.

Ongoing and Future Work

NASA is currently automating the NHATS process in order to provide the most efficient systematic monitoring of NEA accessibility for HSF. A dedicated computer will perform a daily check for NEAs newly added to the SBDB, process them using the algorithms described herein, and add any new results to the growing database of trajectory solutions and vital statistics. An email notification system will be put in place to provide

timely notification of interesting NEAs as soon as the NHATS system identifies them. A website will also be created to provide easy access to trajectory statistics and complete trajectory data and PCC plots for specific NEAs. Once that system is in place, additional features will be added, such as NHATS-style computation of all possible one-way trajectories for scientific and HSF robotic precursor purposes, and re-processing of NEAs when their ephemerides are updated by new observations.

Additional software tools are currently being considered to compliment the NHATS algorithm set. One example is an NHATS-style tool to compute all possible abort trajectory options during the outbound leg of any NEA mission opportunity of interest. The quality of abort options, in conjunction with the quality of robotic precursor opportunities, could serve as an important discriminator between NEAs which otherwise appear to fare equally well in terms of the HSF mission opportunities they offer.

A new software tool currently under construction will automate the process described herein whereby STK/Astrogator is utilized manually to convert a particular NHATS trajectory solution into a fully integrated trajectory within the STK analysis environment. The new tool will use the STK COM interface between MATLAB and STK to allow an analyst to simply compose an input file containing a pointer to the NHATS trajectory solution database, constraints, vehicle parameters, and a host of analysis option flags, and then have the trajectory solution process execute automatically. This tool will be able to quickly compute notionally optimal trajectory solutions with highly detailed analysis, enabling rapid and detailed assessments. STK's built-in modules will permit a host of rapid analyses, including conversion of all impulsive maneuvers to finite burns, sizing of vehicle elements, communications link budget analysis, attitude analysis for vehicle pointing constraints, and even modeling of proximity operations trajectories during the stay time at the NEA.

Finally, the NHATS algorithms are currently being used to study round-trip trajectory dynamics for NEAs in an effort to develop dynamical theories of round-trip accessibility. These efforts are yielding new insights into why certain NEAs are highly accessible compared to others, and which classes of NEA orbit may prove most accessible for HSF. A complimentary line of research currently under consideration is the development of an IMLEO definition that is meaningful even in the context of a currently ill-defined future HSF mission architecture. Such an IMLEO definition has the potential to provide a more relevant metric for assessing relative accessibility for NEAs, which would in turn aid dynamical accessibility theory investigations.

REFERENCES

[1] Barbee, B. W., Esposito, T., Piñon, E. III, Hur-Diaz, S., Mink, R. G., and Adamo, D. R., "A Comprehensive Ongoing Survey of the Near-Earth Asteroid Population for Human Mission Accessibility," *Proceedings of the AIAA/AAS Guidance, Navigation, and Control Conference*, Toronto, Ontario, Canada, 2-5 August 2010. Paper 2010-8368.

[2] Barbee, B. W., ed., *Target NEO: Open Global Community NEO Workshop Report*. 2011. downloadable from URL `http://www.targetneo.org`.

[3] Orloff, R. W. and Harland, D. M., *Apollo: The Definitive Sourcebook*, p. 581. Springer-Praxis, 2006.

[4] Wie, B., *Space Vehicle Dynamics and Control*, pp. 281–2. American Institute of Aeronautics and Astronautics, Inc., 1998.

[5] Chesley, S. R., Chodas, P. W., Milani, A., Valsecchi, G. B., and Yeomans, D. K., "Quantifying the Risk Posed by Potential Earth Impacts," *Icarus*, Vol. 159, October 2002, pp. 423–432. doi:10.1006/icar.2002.6910.